JOURNAL OF CATALYSIS 61, 232–241 (1980)

Deactivation of Alumina-Supported Nickel and Ruthenium Catalysts by Sulfur Compounds[1]

P. W. WENTRCEK, J. G. MCCARTY, C. M. ABLOW, AND H. WISE

Solid State Catalysis Laboratory, SRI International, Menlo Park, California 94025

Received April 9, 1979; revised July 30, 1979

The kinetics of sulfur deactivation of alumina-supported nickel and ruthenium catalysts are examined under methanation conditions in the presence of low concentration of H_2S (<10 ppm) added to the feed stream ($H_2/CO = 4/1$). Based on a theoretical analysis of catalyst deactivation by irreversibly adsorbed surface sulfur atoms, we calculate the deactivation rate constants for the poisoning process. The Ru/Al_2O_3 catalyst exhibits a higher poisoning rate constant than Ni/Al_2O_3. The catalytic properties of Ni/Al_2O_3 are greatly modified by the addition of low concentrations of Ir. The $Ni/Ir/Al_2O_3$ catalyst exhibits higher methanation activity and greater resistance to sulfur deactivation. Temperature-programmed desorption and surface reaction studies indicate the formation of new binding states for CO adspecies on the surface of the Ni/Ir catalyst. Surface composition measurements by means of Auger electron spectroscopy demonstrate considerable Ir enrichment on the surface of the $Ni/Ir/Al_2O_3$ catalyst.

I. INTRODUCTION

Catalytic methanation with nickel-based catalysts represents an important process for the production of substitute natural gas (SNG). However, the use of nickel catalysts requires careful cleanup of the feed gas (removal of sulfur- and halogen-containing compounds as well as organic materials) and control of temperature, because of the catalysts' sensitivity to feed stream impurities and thermal sintering. On a fundamental level the interaction of sulfur compounds with single-crystal nickel surfaces of various orientations has received considerable attention (*1–3*). The dynamics of catalyst poisoning have dealt predominantly with intraparticle mass transfer effects of porous catalysts in the presence of various types of adsorption mechanisms of the deactivating species (*4*).

Studies of reversible chemical adsorption of sulfur on nickel surfaces (*5, 6*) have demonstrated that the enthalpy of formation of the sulfur adlayer is larger in absolute value than the energy of formation of the three-dimensional bulk sulfide Ni_3S_2. The large heat of formation of the surface adlayer demonstrates further that the loss in catalytic activity of a nickel-based catalyst is associated with changes in the surface properties, and does not require the formation of a three-dimensional sulfide. However, for dispersed Ni catalysts no detailed information is available on the relationship between methanation activity, the degree of sulfur surface coverage, and the change in the absorbate binding states. In the present study we examine two Ni-based catalysts, one an alumina-supported Ni catalyst, the other an alumina-supported Ni/Ir catalyst. In addition we present some results on sulfur poisoning of a Ru/Al_2O_3 catalyst. The objective of our research is the evaluation of rate constants for sulfur poisoning of these catalysts under methanation conditions.

[1] Support of this research by the Gas Research Institute is gratefully acknowledged.

0021-9517/80/010232-10$02.00/0

II. EXPERIMENTAL DETAILS

A. Catalysts

A commercial nickel catalyst[2] (25 wt% Ni supported on alumina), in the form of $\frac{1}{8}$-in. extruded pellets, was crushed and screened to a particle size range from 61 to 88 μm (170 to 250 mesh size). Preceding an experimental measurement an aliquot of the powdered catalysts was reduced *in situ* in flowing hydrogen at 1 atm and 723 K over a period of 15 h.

The Ir-promoted catalyst was prepared by impregnation of G-65 with a sufficient quantity of an aqueous solution containing K_2IrCl_6 to deposit 1.0 wt% iridium. For reduction to the metallic phase the catalyst sample was exposed at room temperature to a solution of 5 wt% hydrazine in 0.5 *N* NaOH. Subsequent washing in hot distilled water was carried out until no Cl^- ions were detectable, as monitored by exposure of an aliquot of the wash water to 1 *M* $AgNO_3$. Finally the catalyst samples were reduced in H_2 at 1 atm and 723 K for 15 to 114 h.

The surface composition of the bimetallic catalyst was determined by means of Auger electron spectroscopy (AES) using the $M_5N_7O_4$ (230 eV) transition for Ir, and the $L_3M_{4,5}M_{4,5}$ (850 eV) transition for Ni (*7*). A nearly 10-fold enrichment of Ir near the surface was noted (Table 1). This composition was found to undergo little change during prolonged catalytic reaction.

TABLE 1

Surface Composition of Ni–Ir–Al_2O_3 Catalyst[a] by Auger Electron Spectroscopy

Element ratio	Nominal	Observed
O/Al	1.50	1.50
Ni/Al	1.46	1.42
Ir/Al	0.012	0.19

[a] 25 wt% Ni, 1 wt% Ir; catalyst reduced in H_2 for 115 h at 723 K.

B. Apparatus and Measurements

The experimental measurements employed in this study fell into two categories. One dealt with surface studies of CO interaction with the catalysts in the presence of different degrees of sulfur coverage. For this purpose the techniques of temperature-programmed desorption (*7*, *8*) (TPD) and temperature-programmed surface reaction (TPSR) (*9*) were used. The other involved methanation studies in a differential reactor with feed gas (CO, H_2) containing low concentrations of H_2S.

In the TPD and TPSR experiments the catalyst sample was located in a pulse-flow microreactor. Approximately (10 to 30) $\times$ 10^{-3} g of powdered catalyst was spread uniformly over a fritted glass support (1 cm^2 in cross-sectional area) in a cylindrical glass reactor (3 cm^3 in volume). Helium (in TPD) or hydrogen (in TPSR) at 1 atm was used as carrier gas. Pulses of H_2S (2×10^{-7} to 2×10^{-8} mole) in helium or hydrogen were introduced into the carrier by means of a switching valve located upstream of the reactor. Gases leaving the catalyst bed were continuously analyzed by leaking a small fraction of the reactor effluent into an EAI Quad 300 mass spectrometer system. The sample was indirectly heated by a resistance wire wrapped around a quartz glass tube surrounding the reactor and extending 3 cm above and below it. The reactor could be heated at a linear rate of 0.1 to 1 K s^{-1} from room temperature to 1000 K. A small chromel–alumel thermocouple, 0.005 in. in diameter, in contact with the bed recorded the catalyst temperature. The heating rate was controlled by a programmable temperature controller.

In the continuous-flow methanation studies (space velocities $\leq 1.4 \times 10^5$ h^{-1}) with the differential reactor, the catalyst sample (25 to 50 $\times$ 10^{-3} g) was first reduced *in situ* in 1 atm H_2 at 723 K, and then exposed at 555 $\pm$ 2 K to reactant gas (H_2/CO = 4/1 v/v) containing low concen-

[2] The catalyst carried the designation G-65 and was kindly supplied by United Catalysts, Inc., Louisville, Ky.

trations of H_2S (2 to 10 ppm). Sample aliquots of the product stream were withdrawn at regular intervals for chemical analysis by gas chromatography after removal of water by passage through a trap cooled by a dry ice/acetone mixture (200 K). For the determination of CO, CO_2, and CH_4 concentrations we employed a chromatographic column at 315 K containing Spherocarb (Analabs) and thermal conductivity detection. For separation and quantitative measurement of sulfur compounds (*10*), such as H_2S, COS, and CS_2, a sample aliquot from the reactor efflux passed through a column containing Chromosil-310 (Supelco) at 315 K into the flame photometric detector (Tracor). The differential continuous-flow experiments provided information of the continuous change in catalyst activity in terms of changing methane yield and CO conversion, as well as on the progressive buildup of H_2S in the exit stream.

III. EXPERIMENTAL RESULTS

A. *Surface Studies with TPD and TPSR*

The two catalysts under study exhibited significant differences in the absorption site

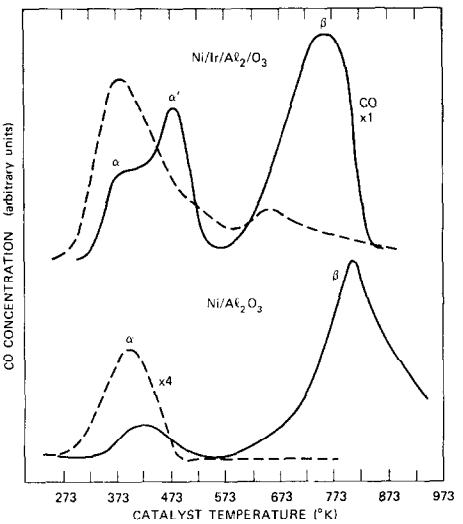

FIG. 1 Temperature-programmed desorption of CO from Ni/Al_2O_3 and $Ni/Ir/Al_2O_3$ with and without surface sulfur. ——, Clean surface; ——, surface exposed to H_2S/H_2. Heating rate = 0.5 K s^{-1}.

TABLE 2

Temperature-Programmed Desorption Spectra of Carbon Monoxide

Catalyst surface	Binding state	Peak desorption temperature (K)[a]	
		Ni/Al_2O_3	$Ni/Ir/Al_2O_3$
Freshly reduced	α-CO	396	368
	α'-CO	—	470
	β-CO	793	753
Exposed to H_2S	α-CO	373	360
	α'-CO	—	—
	β-CO	—	(648)

[a] Heating rate = 0.5 K s^{-1}.

surface density, as measured by CO absorption to saturation coverage at 300 K, and in the CO surface binding energies, as determined in the TPD experiments in which the rate of CO desorption was monitored as a function of temperature. For the Ni/Al_2O_3 catalyst the CO adsorptive capacity corresponded to 6.7×10^{19} CO molecules per gram of catalyst; for the $Ni/Ir/Al_2O_3$ it amounted to 8.6×10^{19} CO molecules per gram of catalyst, an increase of 30%. Typical TPD spectra for the two types of catalysts are presented in Fig. 1. For Ni/Al_2O_3 the desorption rates showed two peaks, a weekly bound state (α-CO) and a more strongly bound state (β-CO) (Table 2). For $Ni/Ir/Al_2O_3$ the TPD data exhibit three binding states (Table 2). It is quite apparent that the intermediate α'-CO binding state is unique to the $Ni/Ir/Al_2O_3$ system, since it is absent from the Ni/Al_2O_3 catalyst (*7*).

Exposure of the Ni/Al_2O_3 catalyst to a number of pulses of H_2S/H_2 sufficient to yield about 75% of saturation surface coverage, as monitored by the "breakthrough" of the H_2S pulse, caused a marked change in the CO binding energy state as compared to the unpoisoned sample. The total amount of CO absorbed was reduced to less than 10% of that on the clean catalysts. In addition the TPD experiment showed the nearly complete disappearance of the high binding energy state (β-CO) in the case of Ni/Al_2O_3 in agreement with the observa-

tions (2) on Ni(111). In the case of $Ni/Ir/Al_2O_3$ the presence of sulfur adspecies greatly attenuated the binding states associated with α'-CO and β-CO, but caused an increase in α-CO (Table 2). For both catalysts the α-CO desorption peaks shifted downward in the presence of sulfur adspecies. It is apparent that surface sulfur greatly reduced the number and binding energy of the CO adsorption sites.

For the clean Ni and Ni/Ir samples the TPD of CO was accompanied by the formation of CO_2 (Fig. 2). Two main peak desorption temperatures were observed (Table 3) for each catalyst. For $Ni/Ir/Al_2O_3$ the total amount of CO_2 formed exceeded that for Ni/Al_2O_3. Irrespective of the mechanism of CO_2 production, either by disproportionation,

$$2CO \rightarrow CO_2 + C_a,$$

or by a sequence of dissociative adsorption and surface reaction,

$$CO_a \rightarrow C_a + O_a,$$
$$CO + O_a \rightarrow CO_2,$$

the catalyst retains an amount of surface carbon equivalent to that of the CO_2 produced. The reactivity of the surface carbon adspecies so formed toward hydrogen represents an important aspect of the methanation mechanism (9). Consequently we carried out a series of TPSR experiments in which we compared the rate of CH_4 formation by reaction of H_2 in the carrier stream with surface carbon, formed by exposure to CO/He pulses at 550 K, and with absorbed CO formed by exposure to CO/He pulses at 300 K. For Ni/Al_2O_3 the TPSR experiment indicates two predominant surface carbon species, as identified by their difference in reactivity toward H_2. A very high rate of methane formation (Fig. 3) is observed at 433 K(C_α), followed by a smaller TPSR peak at 630 K(C_β). The C_α/C_β ratio is about 2, depending on the length of exposure at elevated temperatures preceding the admission of H_2 (11). On the other hand, for CO chemisorbed at 300 K the TPSR data show a single maximum reaction temperature at 475 K. It is of interest to note that the reaction between surface carbon (C_α) and hydrogen occurs at lower temperatures than that of preadsorbed CO with H_2.

For the $Ni/Ir/Al_2O_3$ catalyst the TPSR experiments with H_2 demonstrate somewhat different reaction characteristics (Fig. 4). A single surface carbon species (C_α) is found highly reactive toward H_2, with a maximum in the rate of methane production at 426 K. The C_β species (T_p = 558 K), present in the case of Ni/Al_2O_3, is nearly absent from the surface of the Ir-promoted catalyst (Table 4). For CO chemisorbed at room temperature the maximum rate of methane formation occurs at a somewhat

TABLE 3

Temperature-Programmed Desorption Spectra of Carbon Dioxide

Binding state[a]	Peak desorption temperature (K)[b]	
	Ni/Al_2O_3	$Ni/Ir/Al_2O_3$
α-CO_2/CO	565	506
β-CO_2/CO	783	723

[a] CO_2/CO denotes CO_2 desorption following CO adsorption.

[b] Heating rate: 0.5 K s^{-1}.

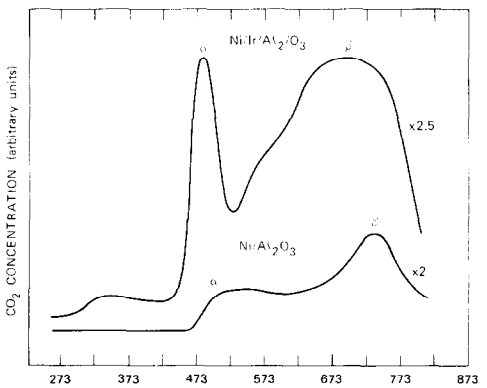

FIG. 2. CO_2 formation during temperature-programmed desorption of CO chemisorbed on Ni/Al_2O_3 and $Ni/Ir/Al_2O_3$. Heating rate = 0.5 K s^{-1}.

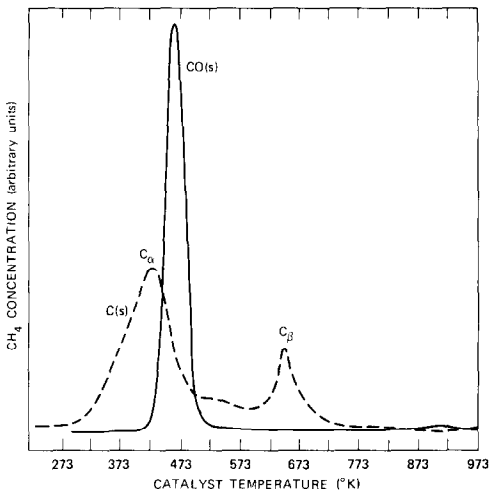

FIG. 3 Temperature-programmed surface reaction with H_2 of chemisorbed CO (——) and surface carbon (——) on Ni/Al_2O_3. Heating rate = 1.0 K s^{-1}.

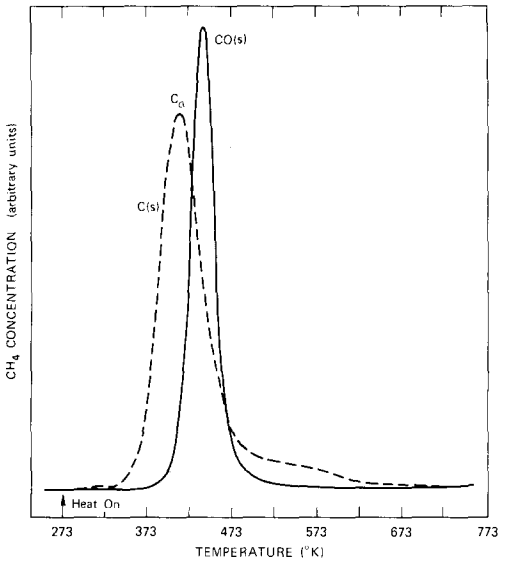

FIG. 4. Temperature-programmed surface reaction with H_2 of chemisorbed CO (——) and surface carbon (---) on $Ni/Ir/Al_2O_3$. Heating rate = 1.0 K s^{-1}.

lower temperature (T_p = 453 K) than observed in the case of Ni/Al_2O_3 (Fig. 3).

Saturation coverage of the $Ni/Ir/Al_2O_3$ catalyst by exposure to H_2S/H_2 pulses[3] and subsequent pulsing with CO/He mixtures at 540 K yielded much lower concentrations of surface carbon (as determined by CO_2 production), about 10% of that found for the clean catalyst. Also this carbon species (C_γ) exhibited very low reactivity toward H_2 as monitored by the peak temperature for methane formation (T_p = 763 K). In the case of Ni/Al_2O_3 preexposed to H_2S/H_2 to saturation coverage, no carbon deposition was detectable.

B. Continuous-Flow Experiments

From the decay of methanation activity during continuous exposure of a catalyst sample to feed gas containing H_2, CO, and low concentrations of H_2S, one can deduce important kinetic parameters on the deactivation process. The theoretical analysis of catalyst deactivation by an irreversibly adsorbed poison is greatly simplified when the contribution of intraparticle and interparticle diffusional transport is negligible. Experimentally the contribution of intraparticle diffusional transport can be diminished by reducing the catalyst particle size. Intra- and interparticle diffusion will vanish under the conditions of low Thiele modulus, high Reynolds number, and a large density ratio of surface sites in the catalyst to poison molecules in the gas phase (as shown in the theoretical analysis presented in the Appendix). In the absence of diffusional limitations the mathematical model allows empirical evaluation of the intrinsic rate constant

TABLE 4

Temperature-Programmed Surface Reaction (TPSR) of Surface Adspecies with Hydrogen[a]

Binding state	Peak TPSR temperature (K)	
	Ni/Al_2O_3	$Ni/Ir/Al_2O_3$
C(α)	433	426
C(β)	630	—
CO[b]	475	453
C(α)/C(β)	~2	>30

[a] Freshly reduced catalyst surface.
[b] Saturation surface coverage at 300 K.

[3] As monitored by the breakthrough of the H_2S pulse.

of catalyst deactivation from measurements of the change in activity of a catalyst caused by progressive occupation of active surface sites with irreversible bound adspecies. In this model the catalyst bed of finite depth L is exposed to the reactant gas mixture at velocity V (space velocity $U = V/L$). The deactivation process involves an irreversibly adsorbed gaseous contaminant of concentration n. As shown in the Appendix the relationship between contaminant density at the inlet (n_i) and the outlet (n_L) of the catalyst bed is found to be

$$\ln[(n_i/n_L) - 1] = \ln[\exp(ks_0/U) - 1] - kn_i[t - (1/U)], \quad (1)$$

where s_0 identifies the initial catalyst site density and t the total exposure time.

Thus from experimental measurements of the variation in outlet concentration of catalyst poison with exposure time, the rate constant k and the site density s_0 can be evaluated. A plot of the quantity on the LHS of Eq. (1) versus the time parameter $[t - (1/U)]$ yields a straight line whose slope is proportional to kn_i, and whose intercept is given by $\ln[\exp(ks_0/U) - 1]$. It will be recognized that the term ks_0/U is the first similarity parameter of Damkohler, defined as the ratio of reaction time to contact time with the catalyst.

A typical time history of the deactivation process for Ni/Al_2O_3 is shown in Fig. 5, in which the concentrations of methane and H_2S in the product stream are plotted as a function of time.[1] The rapid decay in methane formation with sulfur uptake by the catalyst is apparent. Similarly the gradual buildup of H_2S in the reactor efflux is noticeable.

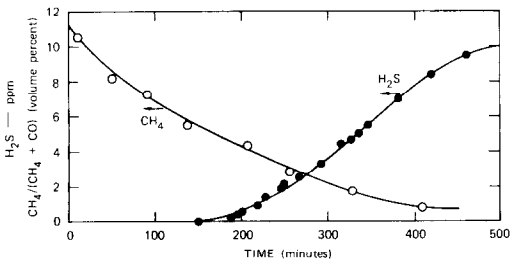

FIG. 5. Chemical composition of reactor efflux. $H_2/CO = 4/1$; $H_2S = 10$ ppm; space velocity = 1.2×10^5 h^{-1}; temperature = 573 K; catalyst = 25 wt% Ni/Al_2O_3.

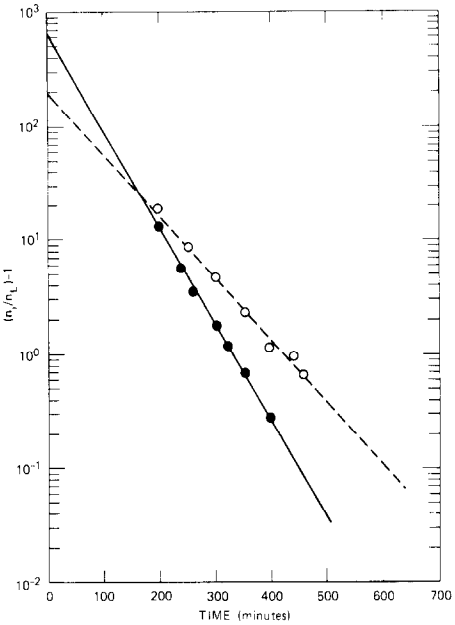

FIG. 6. Kinetics of deactivation by H_2S for Ni/Al_2O_3 (●) and $Ni/Ir/Al_2O_3$ (○) ($H_2/CO = 4/1$; $H_2S = 10$ ppm; space velocity = 2.1×10^5 h^{-1}; temperature = 563 K.

From the graphical analysis of the H_2S data in accordance with Eq. (1), the rate coefficients for catalyst poisoning by H_2S have been evaluated for the two types of Ni catalysts (Fig. 6). Comparison of the values of k (Table 5) demonstrate a 2-fold increase in sulfur resistance brought about by promoting the Ni/Al_2O_3 catalyst with small amounts of Ir. These results were reproducible over a 10-fold variation in space velocity.

Also the analytical model permits calculation of the total number density of acceptor sites s_0 in the catalyst that can be poisoned by sulfur adspecies. From the intercept of the curves presented in Fig. 6

[1] Low concentrations of COS were detectable in the product stream. The COS levels paralleled the H_2S curve but did not exceed 1 ppm.

we calculate the site densities listed in Table 5. The values of s_0 so obtained are somewhat smaller than determined by CO adsorption measurements at 300 K on reduced catalyst samples.

By way of comparison, an Al_2O_3-supported Ru catalyst (5 wt%) exhibited much higher susceptibility to sulfur poisoning as compared to the Ni-based catalysts (Table 5). Although the Ru dispersion was higher, as reflected by the high acceptor site density, the rate constant for deactivation in the case of Ru exceeded that of Ni by a factor of 2, and that of Ni/Ir by a factor of 5.

The decay in the rate of methane formation with H_2S exposure of the Ni/Al_2O_3 catalyst (Fig. 5) appears to be related to the loss in active Ni surface sites. If we assume that methanation activity is proportional to the number density of unpoisoned sites, we find that each S adatom eliminates two sites. Thus the relative loss in CH_4 formation rate is about twice the capture rate of H_2S by the catalyst.

IV. DISCUSSION

The interaction of H_2S with nickel surfaces involves a number of steps including molecular adsorption, dissociative chemisorption, surface diffusion, reconstruction of the sulfur adlayer into a two-dimensional nickel/sulfur compound (*1*), bulk incorporation by dissolution, and finally precipitation of a three-dimensional nickel sulfide phase. Experimental data (*12–15*) indicate rapid dissociative chemisorption of H_2S on nickel at temperatures as low as 175 K. The rapid interaction of H_2S with Ni and the high and constant sticking probability indicate low energy barriers for adsorption, surface diffusion, and dissociation. Thus one might expect that the degree of surface coverage is close to thermodynamic equilibrium at the gas–surface interface.

TABLE 5

Evaluation of Rate Constant for Catalyst Deactivation and Sulfur Acceptor Site Density

Catalyst (wt%)	Deactivation rate constant $((min^{-1} \cdot ppm_{H_2S}^{-1}) \times 10^3)$	Acceptor site density $(g^{-1}\ cat \times 10^{19})$
$25Ni/A_2O_3$	2.0 ± 0.2	6.0 ± 0.6
$25Ni/1Ir/Al_2O_3$	0.8 ± 0.1	8.1 ± 0.8
$5Ru/Al_2O_3$	4.2 ± 0.3	9.1 ± 0.9

Thermodynamic data for chemisorbed sulfur in equilibrium with sulfur in the gas phase (1, 5, 16) suggest a significant exothermic heat of segregation. Recent quantitative measurements (*16*) of reversible adsorption on alumina-supported nickel catalysts including G-65 indicate an equilibrium sulfur activity corresponding to the $H_2S/H_2 < 10^{-2}$ ppb at 600 K near saturation coverage. As a result catalyst surface poisoning occurs at partial pressure ratios of H_2S/H_2 lower by several orders of magnitude than those needed for bulk formation. At 600 K the equilibrium phase boundary for Ni_3S_2 is reached at $H_2S/H_2 = 85$ ppm, well above the H_2S/H_2 levels employed in our measurements.

Surface studies by means of LEED (*1, 17, 18*), indicate the preferential adsorption of sulfur atoms at high coordination sites. For CO adsorption the same sites appear to be involved for Ni(100), but on the other low-index planes the CO admolecules accommodate at lower coordination sites than in the case of sulfur adspecies. The admission of H_2S to a nickel surface covered with CO admolecules results in the displacement of the CO adsorbate by sulfur atoms as observed in infrared absorption studies (*19*).

In addition we have observed that the adsorption of sulfur species causes a transformation of reactive surface carbon to the less reactive carbon form. A measure of this surface deactivation of the carbon intermediate is to be found in the results of the experimental measurements in which a sample of Ni/Al_2O_3 catalyst, after reduction in H_2 at 723 K, was exposed to pulses of CO/He carrier gas at 553 K. From the amount of CO_2 formed, as measured by gas

chromatography, the amount of carbon deposited by dissociative chemisorption of CO was established. After flushing the catalyst with He, the carbon adspecies were exposed to pulses of H_2 and the concentration of CH_4 in each pulse leaving the microreactor was determined by gas chromatography. Quantitative conversion of the surface carbon to methane was noted under these conditions as reported previously (*9*). However, if a pulse of H_2S/He preceded the exposure of the carbon deposit to the hydrogen pulses, the conversion of the surface carbon to methane was progressively reduced (Table 6). The gradual conversion of the active surface carbon to a nonreactive surface species is quite apparent. At the same time it was noted that less and less of the CO pulse dissociatively adsorbed as the nickel surface became populated with the sulfur adsorbate. We are led to conclude that sulfur poisoning of the nickel catalyst is the result of two concurrent effects: (1) preemption of surface sites needed for CO dissociation, and (2) conversion of surface carbon species to a relatively nonreactive form.

The latter effect is demonstrated further in observations made with Auger electron spectroscopy (*20*). Rapid conversion of a surface carbon species with carbidic fine structure to graphitic-type carbon was seen to occur on admission of low concentration

TABLE 6

Deactivation of Surface Carbon by Hydrogen Sulfide on Ni/Al_2O_3 Catalyst[a]

H_2S exposure (moles × 10^7)	Surface carbon (moles × 10^7)		Fractional deactivation of surface carbon (%)
	Deposited[b]	Converted[c]	
0	1.05	1.11	0
0.4	0.95	0.53	44
1.2	0.93	0.32	66
2.4	0.73	0.15	80
3.2	0.42	0.06	86

[a] 15.2×10^{-3} g of Ni/Al_2O_3 (25 wt%).

[b] From pulse of CO (4.86×10^{-6} mole) at 553 K.

[c] Surface carbon converted to CH_4 by exposure to hydrogen pulses.

of H_2S to a nickel surface on which carbon had previously been deposited by exposure to CO. The presence of sulfur adspecies appears to favor the growth of islands of carbon with the formation of carbon-to-carbon bonds and the production of amorphous or graphitic carbon. Undoubtedly this process is caused by reconstruction of the crystallite surface brought about by sulfur.

How does the addition of small concentrations of Ir affect the surface properties of the Ni catalyst? For one we note an increase in site density for CO adsorption, and a change in the distribution of binding states (Table 2). Such a change in surface coordination undoubtedly affects the bonding of sulfur atoms by altering the number density of fourfold and threefold coordinated sites preferred by the sulfur adspecies on a number of crystallographic planes (*18*).

The effect exhibited by the addition of low concentrations of Ir is magnified by the high degree of surface enrichment with Ir, as observed by Auger electron spectroscopy. The large atomic radius of the Ir atom appears to be responsible for surface segregation from the Ni lattice. Reduction in lattice strain is achieved by moving the Ir atom from the lattice interior to the surface (*21*). Based on the known bulk and shear moduli of solute (Ir) and matrix (Ni) we calculate an exothermic heat of segregation of 32 kJ $mole^{-1}$. The Gibb's regular solution model would favor Ni surface enrichment, since its surface free energy is lower than that of Ir. But the opposite effect is noted experimentally.

A series of $Ni/Pt/Al_2O_3$ and $Ni/Pd/Al_2O_3$ catalysts, spanning a range of weight loadings of the respective noble metals, were prepared by the same procedure as employed for $Ni/Ir/Al_2O_3$. However little enhancement in catalytic methanation activity and sulfur resistance was observed. In the Ni/Pd system (Pd $<$ 1 atom%) surface segregation of Pd has been reported (*22*). Similarly Pt would be expected to enrich at the

surface of Ni/Pt. The absence of a homogeneous random bimetallic phase on the surfaces of Ni/Pd or Ni/Pt may be responsible for the absence of a promotional effect. Thus in the case of Ni/Ir not only would the metal atom distribution at the surface be different, but an electronic alloy effect may come into play. Further work is in progress to elucidate the surface properties of these mixed-metal systems.

APPENDIX: THEORETICAL ANALYSIS OF CATALYST DEACTIVATION

In the following analysis we consider the passage of a gas mixture containing reactants and contaminants through a catalyst bed made up of catalyst particles so that all surface sites are in contact with the gas stream. The catalyst bed lies between two cross sections of a tube that holds the flowing gas. The average gas flow is nearly uniform at velocity V (or space velocity $U = V/L$, where L is the bed depth) so that variables, such as the local concentration n of contaminant species, are uniform over each cross section and functions only of the distance x into the bed and the time t. The rate of catalyst deactivation by the contaminant in the feed stream is taken to be of first order in n and the number density s of active sites. The differential equation for convective transport of the contaminant species through the catalyst reads

$$-\left(\frac{\partial n}{\partial t} + V\frac{\partial n}{\partial x}\right) = kns, \qquad \text{(A1)}$$

where k is the rate constant for catalyst deactivation.

The poisoning process is considered to involve a gaseous contaminant species that is irreversibly adsorbed so that the site density is reduced at the rate

$$\frac{\partial s}{\partial t} = -kns. \qquad \text{(A2)}$$

Although the differential system is nonlinear, a general solution can be obtained by changing to the characteristic independent variables

$$\sigma = x/V \quad \text{and} \quad \tau = t - (x/V).$$

Equations (A1) and (A2) become

$$\frac{\partial n}{\partial \sigma} = \frac{\partial s}{\partial \tau} = -kns. \qquad \text{(A3)}$$

The first equality shows that there is a single function whose partial derivatives are n and s. By taking the function to be $(1/k)\ln\varphi$ one obtains

$$n = \frac{1}{k}\frac{\partial \ln\varphi}{\partial\tau} = \frac{1}{k\varphi}\frac{\partial\varphi}{\partial\tau}, \qquad s = \frac{1}{k}\frac{\partial \ln\varphi}{\partial\sigma} = \frac{1}{k\varphi}\frac{\partial\varphi}{\partial\sigma}. \qquad \text{(A4)}$$

The second equality in Eq. (A3) becomes

$$\frac{\partial^2\varphi}{\partial\sigma\partial\tau} = 0,$$

which has the general solution

$$\varphi = P(\sigma) + Q(\tau),$$

where P and Q are arbitrary functions of their arguments. By Eq. (A4)

$$n = \frac{1}{k}\frac{Q'}{P+Q}, \qquad s = \frac{1}{k}\frac{P'}{P+Q}, \qquad \text{(A5)}$$

where the prime denotes the derivative.

Functions P and Q are determined by the auxiliary conditions

$$s = s_0 \quad \text{at } \tau = 0,$$
$$n = n_i \quad \text{at } x = 0 \text{ or } \sigma = 0,$$

where s_0 and n_i are constants. By integration one obtains

$$P(\sigma) = [P(0) + Q(0)]e^{ks_0\sigma} - Q(0),$$
$$Q(\tau) = [P(0) + Q(0)]e^{kn_i\tau} - P(0),$$

so that by Eq. (A5)

$$n = n_i\theta/(\theta + \xi - 1), \qquad \text{(A6a)}$$

$$s = s_0\xi/(\theta + \xi - 1), \qquad \text{(A6b)}$$

where

$$\theta = e^{kn_i\tau} = e^{kn_i[t-(x/V)]}$$

and

$$\xi = e^{ks_0\sigma} = e^{ks_ix/V}.$$

For reduction of experimental data on

the exit stream it is convenient to write Eq. (A6a) in the form

$$\ln[(n_i/n_L) - 1] = \ln(\xi_L - 1) - kn_i[t - (L/V)], \quad \text{(A-7)}$$

where the subscript L denotes values at $x = L$. Thus, from experimental measurements of the concentration of gaseous poison at the inlet and outlet of the catalyst bed, the poisoning rate constant k can be evaluated by graphical means from a plot of the quantity $\ln[(n_i/n_L)-1]$ versus the time parameter $[t - (L/V)]$ (Fig. 1). The latter parameter represents the difference between the total exposure time and the reciprocal space velocity. The slope of the resulting line yields the rate constant k for a given level of gaseous poison in the feed stream. The density of adsorption sites for the poison s_0 can be obtained from the intercept, which by the definition of ξ is given by

$$\ln(\xi_L - 1) = \ln[\exp(ks_0/U) - 1].$$

To identify the governing parameters one may rewrite Eq. (A7) as

$$\ln[(n_i/n_L) - 1] = \ln(\exp D_1 - 1) - (D_1/\beta)(Ut - 1), \quad \text{(A8)}$$

where

$$D_1 \equiv ks_0/U, \qquad \beta \equiv s_0/n_i.$$

Thus the solution for the inlet-to-exit concentration ratio of catalyst poison is a function of the dimensionless time Ut and parameters D_1 and β. Parameter β is the ratio of site density to gas-phase poison concentration, while D_1 is the first similarity parameter of Dammkohler, the ratio of reaction time to contact time.

A striking feature of the time history of the poison concentration in the exit stream is the point of inflexion, identified as the breakthrough time, $t_{1/2}$, that occurs when the concentration of poison in the exit stream is just half that in the feed. From Eq. (A8) with $n_L = n_i/2$,

$$Ut_{1/2} = 1 + (\beta/D_1)\ln(\exp D_1 - 1). \quad \text{(A9)}$$

REFERENCES

1. Perdereau, M., and Oudar, J., *Surface Sci.* **20**, 80 (1970).
2. Erley, W., and Wagner, H., *J. Catal.* **53**, 287 (1978).
3. Bénard, J., *Catal. Rev.* **3**, 93 (1969).
4. Schoubye, P., *J. Catal.* **14**, 238 (1969).
5. Rostrup-Nielsen, J. R., *J. Catal.* **11**, 220 (1968).
6. Oliphant, J. L., Fowler, R. W., Pannell, R. B., and Bartholomew, C. H., *J. Catal.* **51**, 229 (1978).
7. Wood, B. J., and Wise, H., to be published.
8. Cvetanović, R. J., and Amenomyia, L., *In* "Advances in Catalysis" (D. D. Eley, H. Pines, and P. B. Weisz, Vol. 17, p. 103.
9. Wentrcek, P. W., Wood, B. J., and Wise, H., *J. Catal.* **43**, 363 (1976).
10. Green, D. F., and Bydalek, T. J., *Environ. Sci. Technol.* **7**, 153 (1973).
11. McCarty, J. G., and Wise, H., *J. Catal.* **57**, 406 (1979).
12. Saleh, J. M., Kemball, C., and Roberts, M. W., *Trans. Faraday Soc.* **57**, 1771 (1961).
13. Den Besten, I. E., and Selwood, P. W., *J. Catal.* **1**, 93 (1962).
14. Muller, J. C., and Gibert, R., *Bull. Sci. Chem. Fr.*, 2129 (1967).
15. Martin, S., and Imelik, B., *Surface Sci.* **42**, 157 (1974).
16. McCarty, J., and Wise, H., to be published.
17. Edmonds, T., McCarroll, J. J., and Pitkathly, R. C., *J. Vac. Sci. Technol.* **8**, 68 (1971).
18. Demuth, J. E., Jepsen, D. W., and Marcus, P. M., *Phys. Rev. Lett.* **32**, 1182 (1974).
19. Rewick, R. T., and Wise, H., *J. Phys. Chem.* **82**, 751 (1978).
20. Wood, B. J., and Wise, H., to be published.
21. McLean, D., "Grain Boundaries in Metals." Oxford Univ. Press, London, 1957; Polizotti, R. S., and Burton, J. J., *J. Vac. Sci. Technol.* **14**, 347 (1977).
22. Mervyn, D. A., Baird, R. J., and Wynblatt, P., *Surface Sci.* **82**, 79 (1979).